Physica B 636 (2022) 413850

Contents lists available at ScienceDirect

Physica B: Physics of Condensed Matter

journal homepage: www.elsevier.com/locate/physb

DFT, DFTB and TD-DFT theoretical investigations of π-conjugated molecules based on thieno[2,3-b] indole for dye-sensitized solar cell applications

Rahma El Mouhi [a,*], Ahmed Slimi [a], Asmae Fitri [a], Adil Touimi Benjelloun [a,**], Souad ElKhattabi [a,b], Mohammed Benzakour [a], Mohammed Mcharfi [a], Mustafa Kurban [c]

[a] (ECIM), LIMAS, Faculty of Sciences Dhar El Mahraz, University Sidi Mohamed Ben Abdallah, Fez, Morocco
[b] LISA, National School of Applied Sciences, University Sidi Mohamed Ben Abdallah, Fez, Morocco
[c] Department of Electrical and Electronics Engineering, Kırşehir Ahi Evran University, 40100, Kırşehir, Turkey

ARTICLE INFO

Keywords:
DFTB
thieno[2,3-b] indole
TD-DFT
Optoelectronic properties
TiO_2 model

ABSTRACT

In this study, the electrochemical, photovoltaic and absorption properties of the new designed organic sensitizers dyes: Dye-1, Dye-2, Dye-3 and Dye-4 based on Dye-R, of D-π-A architecture, before and after binding to the TiO_2 cluster surface on the ability to inject electrons to the surface. The D donor is the thieno[2,3-b] indole, π-spacer is thiophene, A acceptor is cycnoacrylic acid (CA). The properties were calculated using functional density theory (DFT), time-dependent TD-DFT and the density-functional tight-binding (DFTB) approach. Our study also focused on the analysis of the effects of the introduction of the auxiliary donor (D′)/acceptor (A′) groups on the main photovoltaic properties of the reference molecule Dye-R and to study the relationship between the molecular structure and optoelectronic properties. The analysis of the calculated properties of the new designed compounds D-D′-π-A (Dye-1), D-π-D′-A (Dye-2), D-A′-π-A (Dye-3) and D-π-A′-A (Dye-4), where A′ is benzothiadiazole and D′ is 9,9-diethyl-9H-fluorene, indicate that the molecular architecture has a significant effect on various properties of the studied dyes and that nature (donor D ′or acceptor A′) of the introduced groups, as well as the choice of their locations with respect to the π bridge, is of great importance. Indeed, among the four designed compounds Dye-4 (D-π-A′-A) and Dye-3 (D-A′-π-A) display significantly better properties than those of the reference molecule Dye-R (D-π-A) and of the two other designed dyes Dye-1 (D-D′-π-A), Dye-2 (D-π-D′-A).

1. Introduction

Massive research efforts have been devoted to Dye-Sensitized Solar Cells (DSSCs) [1–4]. Although DSSCs based on Ru-photosensitizers have reached interesting solar-to-electrical power conversion efficiency values of 11%, [5–10] organic materials based on π-conjugated molecules have become more interesting in much recent research for their use in photovoltaic cells [11,12] in view of their low cost, lightness of their weight and ease of their flexibility as well as having the best performance compared to Si-based and Ru-based solar cells [13,14]. Generally, DSSC systems are formed from a semiconductor (typically TiO_2) sensitized by molecular dyes, capable of capturing light in the visible region in the presence of a redox electrolyte (iodide/triiodide I^-/I^-_3) [15,16]. In the DSSC, the incoming light causes electronic excitations of sensitized dyes leading to the injection of electrons to the conduction band of the nanocrystalline metal oxide, then, the dyes take up the electrons of the redox couple that exists in the solution electrolyte [17]. These molecular dyes can produce electricity if at least two conditions are met, the energy of its highest occupied molecular orbital (HOMO) must be below the HOMO energy of the electrolyte to accept electrons from a pair of redox electrolytes (such as I^-/I^-_3) and its lowest unoccupied molecular orbital (LUMO) must have higher energy than that of the semiconductor conduction band (TiO_2). Most studied organic dyes are simulated with a donor-π-acceptor structure (D-π-A) [18]. In this structure, the intramolecular charge transfer (ICT) from the donor to the acceptor generates the photoexcitation that will occur during the transfer of electrons to the conduction band of the semiconductor through the acceptor moiety. Many metal-free organic dyes, such as

* Corresponding author.
** Corresponding author.
E-mail addresses: rahma.elmouhi@usmba.ac.ma (R. El Mouhi), touimiba@gmail.com (A.T. Benjelloun).

https://doi.org/10.1016/j.physb.2022.413850
Received 15 December 2021; Received in revised form 7 March 2022; Accepted 15 March 2022
Available online 24 March 2022

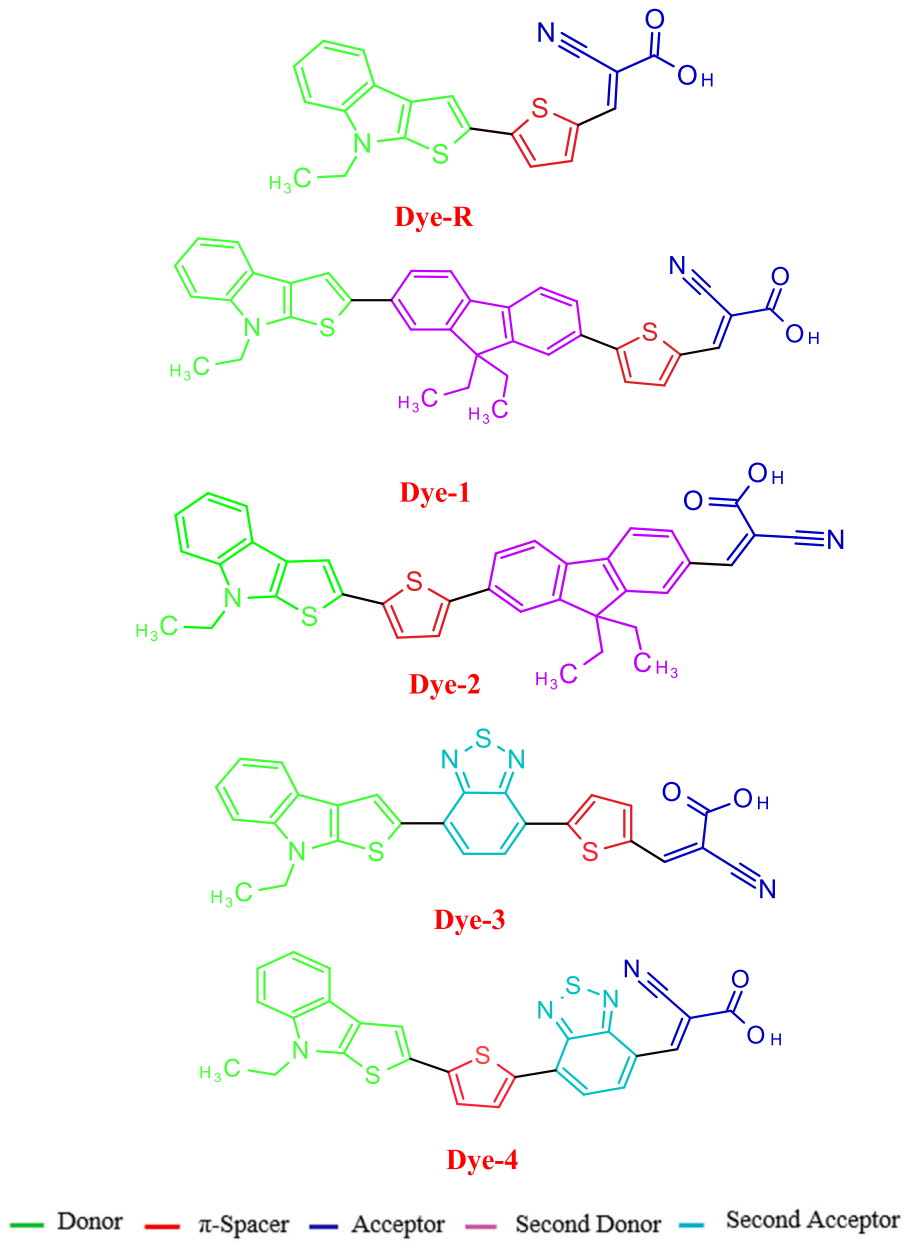

Fig. 1. Chemical structures of the studied dyes (Dye-R, Dye-1, Dye-2, Dye-3 and Dye-4).

Triphenylamine [19–21], indoline [22,23] have been reported as efficient sensitizers for DSSCs. In 2015, Irgashiv et al. [24] have synthesized a series of two dyes (IK-1 and IK-2) with a configuration of D–π–A, for use in dye-sensitized solar cells. Additionally, the power conversion efficiency (PCE) of the synthesized compounds reached 6.3%. Recently, many theoretical studies based on these dyes (IK-1 and IK-2) have given good results [25–28]. Motivated by these results, we intend to investigate the effects of the molecule architecture (D-π-A, D-D′-π-A, D-π-D′-A, D-A′-π-A and D-π-A′-A) (Fig. 1) on the geometric, electronic and optical properties, in order to establish the relationship between the chemical structure and device performance. Where, the thieno [2,3-b] indole is employed as the donor, thiophene as a π-bridge unit, cyanoacrylic acid (CA) as acceptor moiety which has been commonly used as anchoring group due to its interesting electron-injection property and the increased spectral response based on a strong intramolecular charge transfer (ICT) [29–31], D′ is 9,9-diethyl-9H-fluorene [32] used as the second donor and A′ is benzothiadiazole [33] used as the second acceptor. Finally, to see the influence of electron transfer between dyes and TiO_2, we attached dyes to the cluster $(TiO_2)_8$ and performed theoretical calculations using Dmol^3 software.

2. Theoretical methodology

All the quantum calculations of the DFT method and its TD-DFT approach were performed with the Gaussian 09 program [34] supported by the GaussView 5.1.8 interface [35]. The geometrical structure of the compounds has been optimized at the electronic ground state (S0) using the hybrid functional Becke three parameters B3 with the nonlocal correlation of Lee-Yang-Parr LYP named B3LYP, combined with the 6-31G (d,p) basis set. We also used a semi-empirical method the method of Density-Functional Based Tight-Binding (DFTB) which makes it possible to treat systems more than ten atoms and which gives very interesting results [36,37]. So, the electronic properties have also been investigated using DFTB calculations in DFTB + code [38] with the mio-1-1 [39,40] set of Slater-Koster parameters. The Natural Bond Orbital (NBO) [41] analysis has also been investigated by the calculated

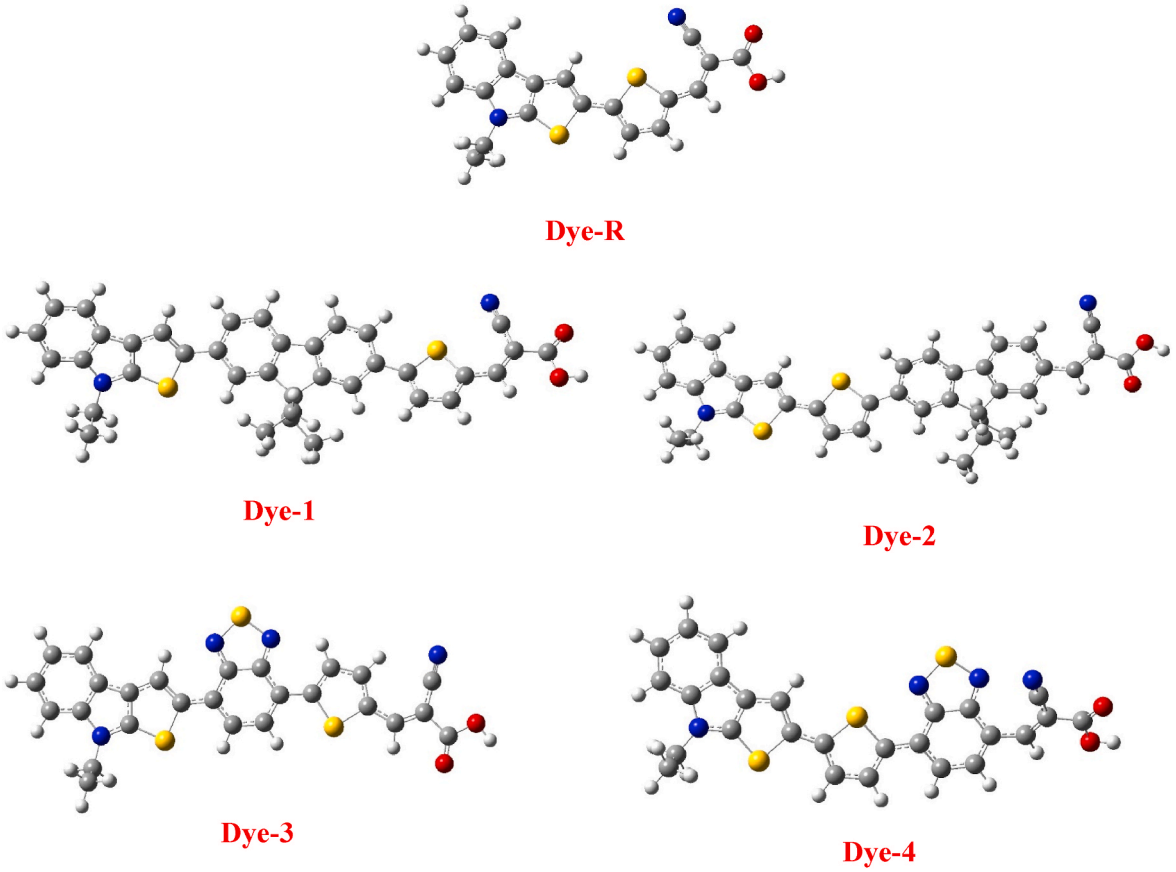

Fig. 2. Optimized geometry obtained by B3LYP/6-31G(d,p) for all dyes.

Table 1
Selected dihedral angle Φ (∘) and distances d (Å) of studied compounds.

Dye		*d (Å)*	*Φ (°)*
Dye-R	*D-π*	1.44	179.50
	π-A	1.42	179.93
Dye-1	*D-D′*	1.46	154.42
	D′-π	1.46	157.49
	π-A	1.43	179.12
Dye-2	*D-π*	1.44	166.94
	π-D′	1.46	158.52
	D′-A	1.45	179.79
Dye-3	*D-A′*	1.45	179.53
	A′-π	1.45	178.57
	π-A	1.43	179.99
Dye-4	*D-π*	1.44	175.78
	π-A′	1.45	175.78
	A′-A	1.45	151.59

Note.
D is donor: Thieno[2,3-b] indole.
π-linker: Thiophene.
A is acceptor: Cyanoacrylic acid.
D′ is second donor: 9,9-dimethyl-9H-fluorene.
A′ is second acceptor: Benzothiadiazole.

orbital populations using NBO 6.0 program implemented in the Gaussian software. Furthermore, the electronic density of states (DOS) was performed by GaussSum package [42] with B3LYP/6-31G (d, p) method. Indeed, The excitation energy, optical properties, oscillator strength, and including ultraviolet–visible (UV–Vis) spectrum were obtained by TD-DFT calculations using the CAM-B3LYP [43,44] with the integral equation formalism polarizable continuum model (IEF–PCM) [45,46] in chloroform ($CHCl_3$) to evaluate the solvent effect in the order to predict the experimental spectra with reasonable accuracy. We chose this functional because it gave more reliable and accurate results and has been used in several recent studies [47–49]. To model the adsorption of the dyes studied on the surface $(TiO_2)_8$ of anatase (101) were performed using a $DMol^3$ package implemented in Materials Studio [50,51]. The optimization of complex dye@$(TiO_2)_8$ were optimized using the generalized method Perdew-Burke-Ernzerhof (PBE) [52] Generalized Gradient Corrected Approximation Method (GGA) functional with the double base set digital polarization (DNP) which is the highest quality base set available in $DMol^3$ [53]. On the other hand, the TD-CAM-B3LYP/6-31G (d, p) level was used to understand the different effects of the addition of auxiliary donors and acceptors on the optical properties of the cluster dye@$(TiO_2)_8$.

3. Results and discussion

3.1. Optimized ground-state geometries

The optimized geometries of all dyes (Dye-R, Dye-1, Dye-2, Dye-3, and Dye-4) obtained using B3LYP/6–31G (d,p) method are shown in Fig. 2. The first, to study the structural properties of these five thieno [2,3-b] indole-based dyes, we determined the two parameters, dihedral angles **Φ**(∘) and bond distances **d** (Å) from the optimized structures (Table 1). All compounds, thieno [2,3-b] indole and cyanoacrylic acid (CA) act as donor and acceptor respectively. For Dye-1 (D–D′-π–A) and Dye-2 (D–π–D′-A), the 9,9-dimethyl-9H-fluorene used as second donor. For Dye-3 (D–A′-π–A) and Dye-4 (D–π–A′-A), the benzothiadiazole used as second acceptor. The obtained bond lengths (d) for all dyes range from 1.42 to 1.46 Å. These values are sufficient for an electron transfer from the donor (thieno [2,3-b] indole) to the acceptor (cyanoacrylic acid). From Table 1, we remark that Dye-R is almost planar (~180°) and after adding the 9,9-dimethyl-9H-fluorene between the donor and the

Table 2
Comparison of energy values (eV) of HOMO, LUMO and energy gap (E_g) for the studied molecules calculated at the DFT/B3LYP/6-31G (d, p) level, DFTB with mio-1-1 set of Slater-Koster parameters and the experimental values.

Dye	*DFT*			*DFTB*			*Exp.* [24]		
	E_{HOMO}	E_{LUMO}	E_g	E_{HOMO}	E_{LUMO}	E_g	E_{HOMO}	E_{LUMO}	E_g
Dye-R	−5.282	−2.573	2.709	−5.151	−3.442	1.709	−5.6	−3.4	2.2
Dye-1	−5.033	−2.632	2.175	−5019	−3574	1.445	–	–	–
Dye-2	−4.931	−2.543	2.401	−4.888	−3.442	1.446	–	–	–
Dye-3	−5.216	−3.041	2.388	−5.099	−3.906	1.193	–	–	–
Dye-4	−5.171	−3164	2.00	−5.048	−3.916	1.132	–	–	–

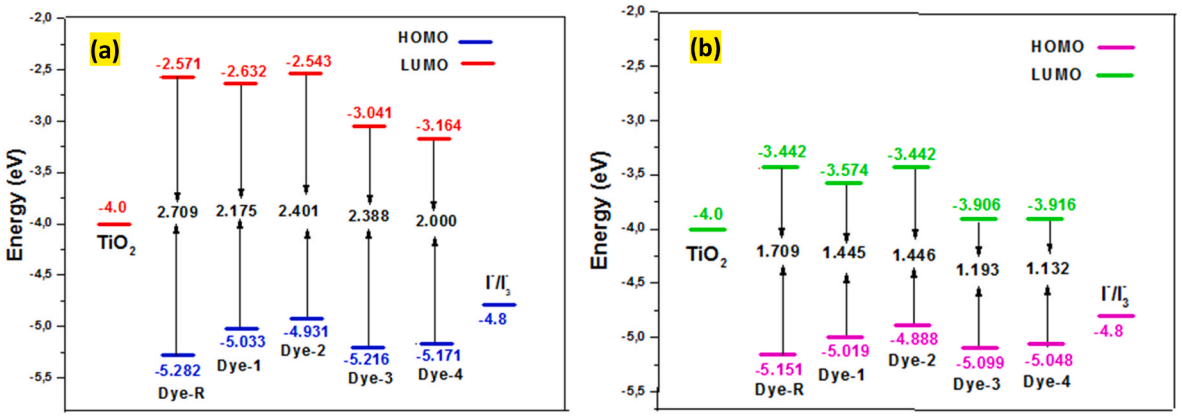

Fig. 3. Schematic energy diagram using DFT (a) and DFTB (b) of all dyes, TiO_2 and electrolyte.

π-linker or between the π-linker and the acceptor, the dihedral angle slightly decreases to almost 154°. Similar constatation has been made after adding the benzothiadiazole between the π-linker and the acceptor (Dye-4), the dihedral angle has decreased. Whereas, the incorporation of the benzothiadiazole between the donor and π-linker (Dye-3) allow to maintain the planar conformation in the whole molecule. These results

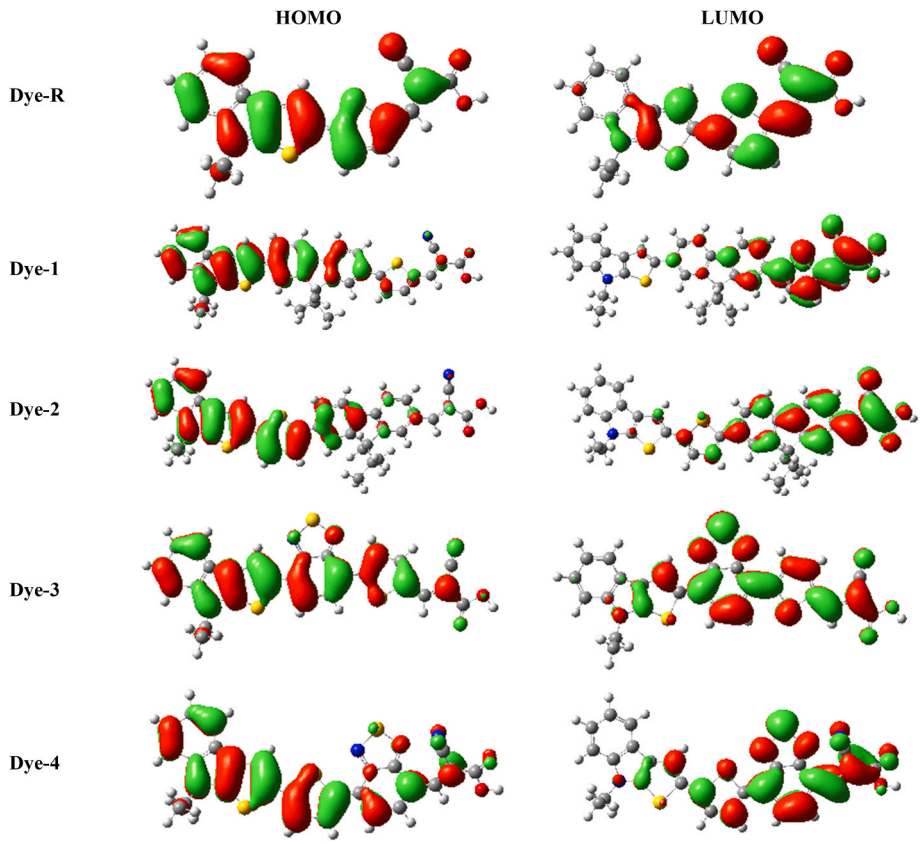

Fig. 4. The contour plots of HOMO and LUMO orbitals of all dyes by DFT/B3LYP/6-31G(d,p).

Table 3
The NBO analysis (atomic charge) of all compounds (in a.u) calculated at the DFT/B3LYP/6–31G (d,p) level.

Dye	D	π-linker	A	D′	A′	Δ(D-A)
Dye-R	0.118	0.054	−0.178	–	–	0.296
Dye-1	0.041	−0.091	−0.151	0.421	–	0.192
Dye-2	0.271	−0.013	−0.124	0.089	–	0.395
Dye-3	0.140	0.120	−0.160	–	−0.107	0.300
Dye-4	0.610	0.056	−0.095	–	−0.052	0.705

Note.
D is donor: Thieno[2,3-b] indole.
π-spacer: Thiophene.
A is acceptor: Cyanoacrylic acid.
D′ is second donor:9,9-dimethyl-9H-fluorene.
A′ is second acceptor: Benzothiadiazole.

show that Dye-3 has the best charge transfer.

3.2. Electronic properties and frontier molecular orbitals (FMO)

The theoretical knowledge of the energy levels of the highest occupied molecular orbital (HOMO) and the lowest unoccupied molecular orbital (LUMO) is crucial to study organic solar cells such as determining if the charge transfer between the donor and acceptor is effective [54, 55]. The calculated values of the HOMO, LUMO and corresponding energy gap E_{gap} obtained from DFT calculations at B3LYP/6-31G (d, p) level and DFTB/the mio-1-1 set of Slater-Koster parameters are summarized in Table 2 and given in Fig. 3. The first, we remark that the energy gap obtained with the DFTB is quite similar to the values obtained from experiment with an acceptable margin of error. We notice also, the energy gap values have decreased when adding second donor or acceptor to the dye-R in the order Dye-R (2.709 eV)> Dye-2 (2401 eV)> Dye-3 (2.388 eV)> Dye-1 (2.175 eV) > Dye-4 (2.000 eV) using DFT and in order Dye-R (1.709 eV)> Dye-2 (1.446 eV)> Dye-1 (1.445 eV)> Dye-3 (1.193 eV) > Dye-4 (1.132 eV) using DFTB. On the other hand, for Molecular Architecture it is important to note that the addition of the benzothiadiazole between the π-linker and the acceptor predicted the smallest value of the energy gap which makes the corresponding dye (Dye-4) to have outstanding photophysical properties. Moreover, we can see in Fig. 3 that the LUMO levels of all dyes are higher than that of the conduction band of TiO_2 (−4.0 eV [56–59]). Whereas, the HOMO energy levels of all dyes are lower than that of the redox couple I^-/I^-_3, which suggests that the photoexcited electron transfer from all dyes to TiO_2 is efficient. So, the decrease of the HOMO level induced by the introduction of the 9,9-diethyl-9H-fluorene as the second donor in Dye-1 and Dye-2, and induced by the introduction of the Benzothiadiazole as the second acceptor in Dye-3 and Dye-4. However, the introduction of Benzothiadiazole in Dye-3 and Dye-4 stabilizes the LUMO. This suggests that adding a Benzothiadiazole as the second acceptor in Dye-3 and Dye-4 improves the efficiency of electron injection into TiO_2. Finally, we can conclude that we notice a better transfer of charge using the DFTB method because the DFTB method allows a considerable gain in computing time by the simplicity of its formalism and the parameters used. It is also suitable for the description of large atom systems, which is limited in DFT method.

In DSSC, the HOMO and LUMO orbitals play an important role in understanding the physicochemical properties behavior of all chemical compounds [60]. In this context, we have determined from the optimized structures, the distribution of the electron density of the studied dyes using the DFT/B3LYP/6-31G(d, p) method. As shown in Fig. 4, the HOMO is delocalized over the whole molecule Dye-R, Dye-3 and Dye-4 but for Dye-1 and Dye-2 the HOMO is mainly contributed by the donor (D), while LUMO is mainly distributed on the acceptor for all dyes, suggesting large orbital overlap between HOMO and LUMO.

3.3. Natural bond orbital (NBO) analysis

Based on the optimized geometries of the ground state for all dyes, we calculate the natural bond orbital (NBO) analysis to understand the electron transfer mechanism [61]. The calculated values of NBO are presented in Table 3. The analysis of the calculated results of the NBO charges of the electron donor, thieno [2,3-b] indole, of the Dye-R, Dye-1, Dye-2, Dye-3 and Dye-4, 0.118, 0.041, 0.271, 0.140 and 0.610

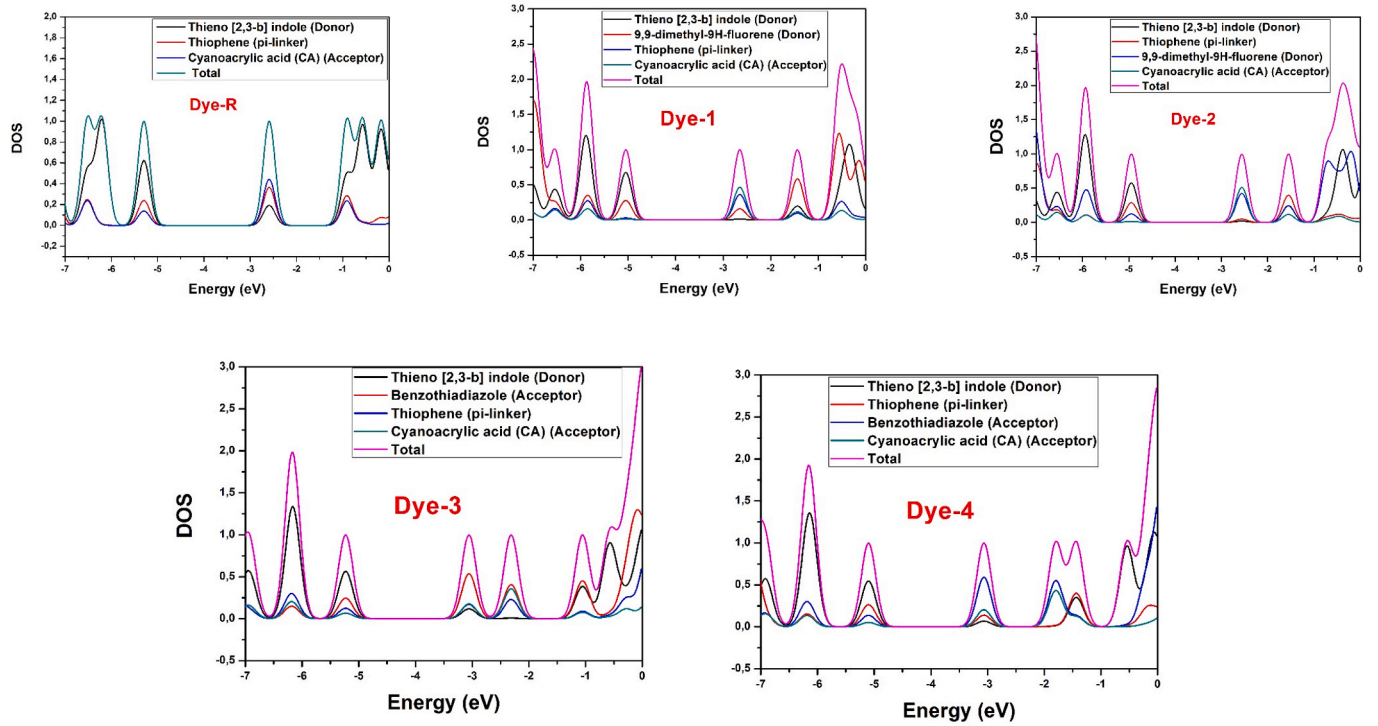

Fig. 5. HOMO, LUMO, and density of states (DOS) of all dyes.

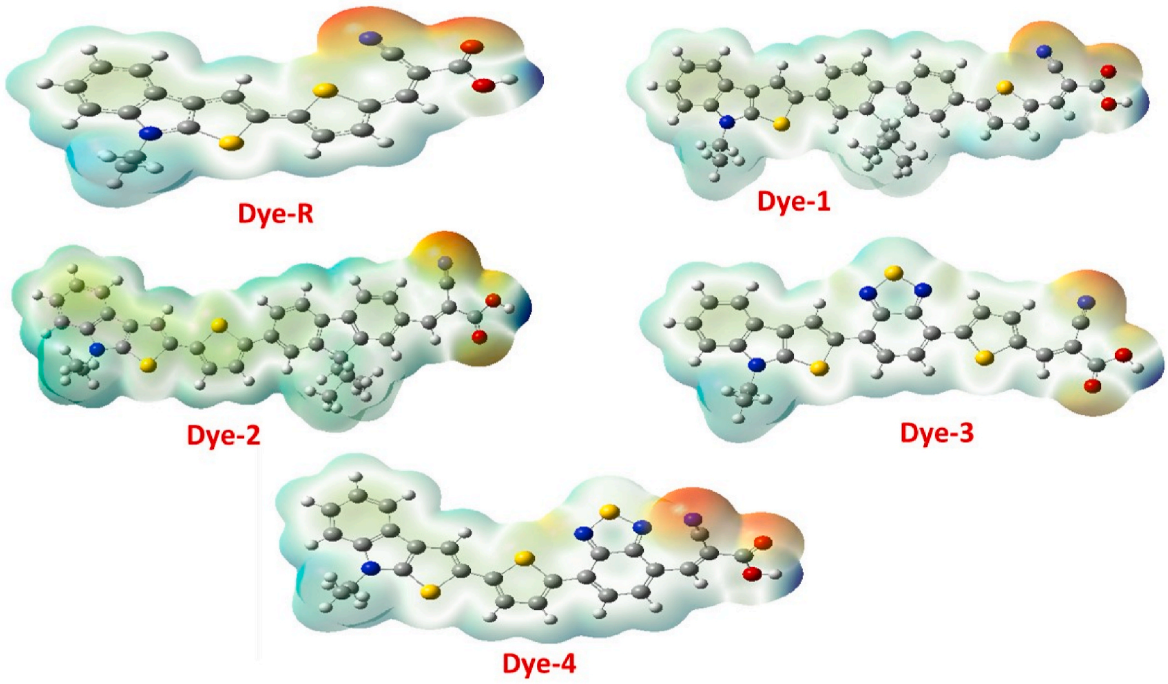

Fig. 6. The calculated Molecular electrostatic potential (MEP) and reactivity for all dyes.

respectively, indicate that the all calculated values are positives, which means that thieno[2,3-b] indole is an effective electron pushing unit. We also note that the thieno[2,3-b] indole in the Dye-4 (0.610) exhibits a strong electron pushing ability comparing with the other dyes. Additionally, the NBO charges of the electron donor, thieno [2,3-b] indole Dye-2>Dye-1 and Dye-4>Dye-3, while, the position of thiophene affects the donor character of the indole. This donor character is important when thiophene is linked to indole. On another side, the negative charges in the acceptor group may trap the electron in the molecular backbone. To the π-spacer, we remark that the NBO charges for the five dyes can be either positive (Dye-R, Dye-3 and Dye-4) or negative (Dye-1 and Dye-2). It appears that the incorporation of the auxiliary donor, 9, 9-diethyl-9H-fluorene, modified the electron-donating character of the π-spacer in the Dye-R. Finally, we note also good charge-transfer Δ(D-A) in the Dyes (Dye-2 and Dye-4) when the π-spacer is directly linked with the donor (thieno [2,3-b] indole), indicate that these architectures of these dyes allow an effective charge transfer from the dyes to the TiO_2 when these structures are used in DSSC solar cells.

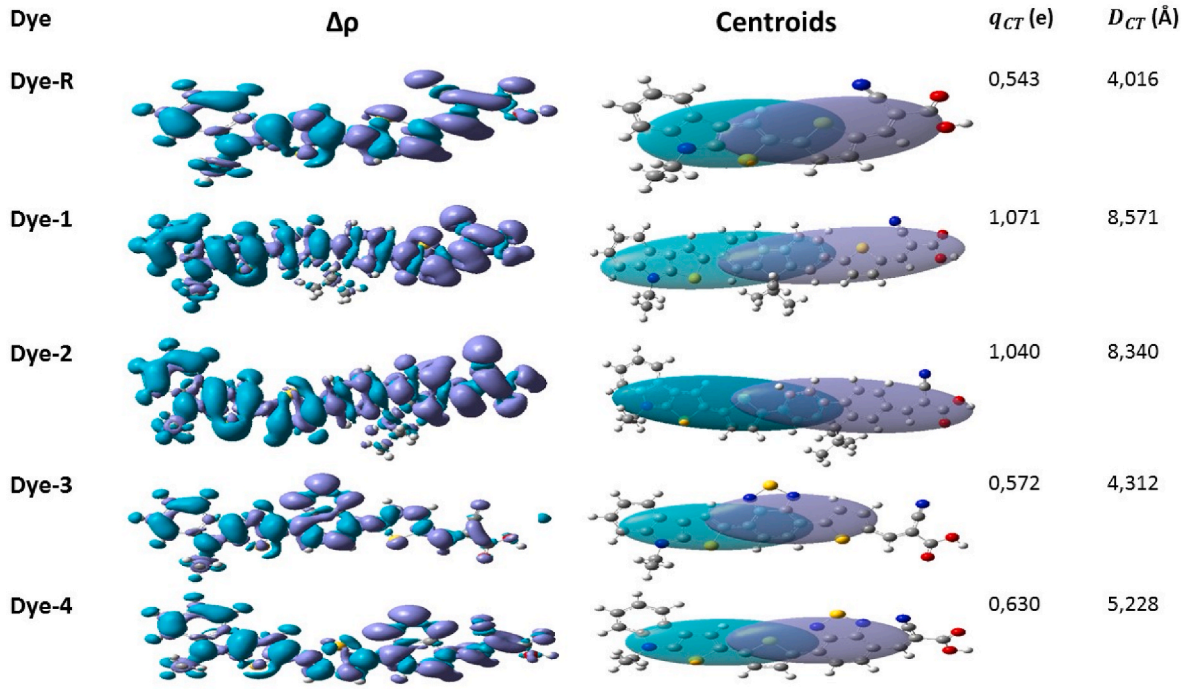

Fig. 7. Plots of the frontier molecular orbitals under B3LYP/6-31G(d,p), charge density difference (Δρ) maps, between the ground state and the first excited state with an isodensity of 0.005 au and centroids of charges for all dyes and the computed charge transfer parameters (q_{CT} in |e−| and D_{CT} in Å) in chloroform.

3.4. Density of states (DOS) analysis

The (DOS) is used to determine the charge transport properties of any materials [62]. In addition, DOS calculations are particularly useful to investigate the energies of all the occupied as well as unoccupied MOs of the dyes. The calculated density of states plots and illustrated in Fig. 5 were performed using GaussSum software. The analysis of these plots shows that the DOS of the five studied dyes are almost identical. In addition, we remark that this density of states is in good agreement with the FMO study (Fig. 4). DOS has also shown that HOMOs are mainly located on the thieno[2,3-*b*]indole donor, and LUMOs are essentially from the cyanoacrylic acid acceptor. Finally, we can clearly see from DOS that the lowest energy gap value is that of Dye-4.

3.5. Molecular electrostatic potential (MEP)

The molecular electrostatic potential (MEP) is directly related to electron density and a very useful descriptor in detecting sites for electrophilic and nucleophilic attack reactions, as well as hydrogen bond interactions [63,64]. The MEP was evaluated using the DFT/B3LYP/6-31G (d) method (Fig. 6). In addition, this figure shows the electrostatic potential values using a color-coded diagram. The most negative value is characterized by red, which suggests the prime sites for possible electrophilic attack. The most positively charged regions appear in dark blue, which in turn indicates favorite sites for nucleophilic attack. To further, the most negative potential is concentrated around the nitrogen atom and the oxygen which means that this area is favorable for electrophilic attacks. While the positive potentials are peripheral, in particular at the level of the H atoms of the acceptor CA indicating that this area is adequate for nucleophilic attacks.

3.6. Intramolecular charge transfer (ICT) properties

The intramolecular charge transfer (ICT) is one of the most important characteristics in DSSCs from the donor group to the acceptor group between the first excited state and the ground state [65]. As is known, the blue and purple colors represent the regions where the electrons come from and where the electrons go. To further, the blue color shows the decrease in electron density and the purple color indicates the increase in electron density. As shown in Fig. 6, the blue color is mainly localized on the donor (thieno [2,3-b] indole) of all dyes. While the purple color is mainly localized on the acceptor parts (CA) of all dyes except in Dye-3 and Dye-4 molecules where it is concentrated on the π-linker (Thiophene) and the second acceptor (Benzothiadiazole). This meant that localized electron densities showing that electron charge transfers occur in the donor (This meant that localized electron densities showing that electron charge transfers occur in the donor (9,9-diethyl-9H-fluorene) to acceptor direction except) to acceptor (CA) direction except in Dye-3 and Dye-4 colorants where electron charge transfers pass from donor to the second acceptor (Benzothiadiazole).

In the same way and to understand more about the intramolecular charge transfer (ICT), we calculated the transferred charge (q_{CT}) and the spatial distance (D_{CT}). The results are presented in Fig. 7.

$$q_{CT} = \int \rho_{+}(r)dr = \int \rho_{-}(r)dr \tag{1}$$

where $\rho_{+}(r)$ and $\rho_{-}(r)$ are increment and depletion of the density. The barycenters of density distribution corresponding to $\mathbf{r}_{+}$ and $\mathbf{r}_{-}$ can be expressed as:

$$r_{+} = (x_{+}, y_{+}, z_{+}) = \frac{1}{q_{CT}} \int r\rho_{+}dr \tag{2}$$

$$r_{-} = (x_{-}, y_{-}, z_{-}) = \frac{1}{q_{CT}} \int r\rho_{-}dr \tag{3}$$

Table 4
Energy values (in eV) of LUMO (E_{LUMO}), HOMO (E_{HOMO}) and the open circuit voltage V_{oc} (in eV) of the studied compounds obtained by B3LYP/6-31G (d,p) level.

Dye	DFT			DFTB		
	E_{HOMO}	E_{LUMO}	V_{OC}	E_{HOMO}	E_{LUMO}	V_{OC}
Dye-R	−5.282	−2.573	1.427	−5.151	−3.442	0.558
Dye-1	−5.033	−2.632	1.368	−5019	−3574	0.426
Dye-2	−4.931	−2.543	1.457	−4.888	−3.442	0.558
Dye-3	−5.216	−3.041	0.959	−5.099	−3.906	0.094
Dye-4	−5.171	−3.164	0.836	−5.048	−3.916	0.084
TiO_2	–	−4.000	–	–	−4.000	–

The spatial distance (D_{CT}) can be denoted by distance between two barycenters $\mathbf{r}_{+}$ and $\mathbf{r}_{-}$, which is described as:

$$D_{CT} = |r_{+} - r_{-}| \tag{4}$$

From Fig. 7, we notice that the spatial distance values (D_{CT}) are increased in the following order Dye-R (4.016 Å) <Dye-3 (4.312 Å) <Dye-4 (5.228 Å) <Dye-2 (8.340 Å) <Dye-1 (8.571 Å) This means that the introduction of 9,9-diethyl-9H-fluorene as a second donor in Dye-1 and Dye-2 would have a crucial effect in TIC. On the other hand, the values of the transferred charge q_{CT} are increased in the following order Dye-R (0.543 e^{-}) <Dye-3 (0.572 e^{-}) <Dye-4 (0.630 e^{-}) <Dye-2 (1.040 e^{-}) <Dye-1 (1.071 e^{-}) these results confirm that the introduction of 9,9-diethyl-9H-fluorene as a second donor in Dye-1 and Dye-2 would have the best charge transfer performance and has higher efficiency.

3.7. Photovoltaic properties

The power conversion efficiency (PCE or η) is the most used parameter to study the photovoltaic properties. It is calculated through the open-circuit voltage (V_{oc}), fill factor (FF), short-circuit current (J_{sc}) and incident power density (P_{in}) using Eq. (5) [66]:

$$\eta = \frac{J_{sc} V_{oc} FF}{P_{in}} \tag{5}$$

The open-circuit voltage V_{oc} is among the parameters influences on the efficient of solar cells, the theoretical values of V_{oc} is calculated from the following expressions Eq. (6) [67]:

$$V_{OC} = E_{LUMO}\ (Donor) - E_{CB}\ (TiO_2) \tag{6}$$

where E_{LUMO} is the lower unoccupied molecular orbital of the dyes and E_{CB} is the conduction band of the semiconductor TiO_2.

The V_{oc} values of the studied dyes, calculated using equation (6), vary from 0.836 eV to 1.457 eV using the DFT and 0.084 eV–0.558 eV using the DFTB (Table 4). These values are positive for all dyes, indicating that electron transfer will be easy for the donor (Dye-R, Dye-1, Dye-2, Dye-3 and Dye-4) to TiO_2 semiconductor. Moreover, we conclude that these obtained values are sufficient for a possible effective injection of electrons [68].

3.8. Free energy change for the electron injection and light harvesting efficiency (LHE)

The calculation details for the free energy for electron injection into the conduction band of the semiconductor surface (TiO_2) for all dyes were calculated using Eq. (7) [69]:

$$\Delta G^{inject} = E_{ox}^{dye*} - E_{CB} \tag{7}$$

where E_{CB} is the reduction potential of the conduction band of TiO_2 (E_{CB} = −4.0 eV), and E_{ox}^{dye*} is the oxidation potential energy of the dye in the excited state, reported in some papers and expressed as Eq. (8) [70]:

$$E_{ox}^{dye*}(eV) = E_{ox}^{dye} - \Delta E \tag{8}$$

Table 5
Values of photovoltaic parameters of studies dyes obtained with B3LYP/6-31G (d, p) level.

Dye	$E_{ox}^{dye}(eV)$	*ΔE (eV)*	$E_{ox}^{dye*}(eV)$	ΔG^{inject} *(eV)*	*f*	*LHE*
Dye-R	5.282	2.457	2.825	−1.175	1.013	0.903
Dye-1	5.033	2.255	2.778	−1.222	0.881	0.868
Dye-2	4.931	2.239	2.692	−1.308	0.991	0.898
Dye-3	5.216	1.942	3.274	−0.726	1.286	0.948
Dye-4	5.171	1.826	3.345	−0.655	1.097	0.920

Table 6
The energy values of the total reorganization energy (λ_{total}), the reorganization energy the electron (λ_e) and hole (λ_h), the ionization potential (IP) and the electron affinity (EA).

Dye	λ_e (eV)	λ_h (eV)	λ_T (eV)	IP (eV)	EA (eV)
Dye-R	0.320	0.268	0.588	6.416	1.375
Dye-1	0.331	0.282	0.613	5.976	1.565
Dye-2	0.283	0.307	0.590	5.883	1.505
Dye-3	0.270	0.242	0.512	6.196	2.024
Dye-4	0.239	0.235	0.474	6.165	2.080

where ΔE is the vertical excitation energy and E_{ox}^{dye} is the oxidation potential energy of the dye in the ground state.

Efficient sensitizers for DSSCs should have large light-harvesting efficiency (LHE), it can be calculated by Eq. (9) [71]:

$$LHE = 1 - 10^{-f} \tag{9}$$

where f is the oscillator strength of the dye associated with λ_{max}.

The most important parameters of DSSCs based on Dye-R, Dye-1, Dye-2, Dye-3 and Dye-4 determined in the present study are the E_{ox}^{dye}, E_{ox}^{dye*}, ΔG_{inject} and LHE. The obtained results are presented in Table 5.

The E_{ox}^{dye*} values calculated for the studied dyes increased in the following order: Dye-R < Dye-2<Dye-1<Dye-3<Dye-4, indicating that Dye-4 is the least oxidizing while Dye-R is the most oxidizing compound among these dyes. For the free energy change (ΔG^{inject}) while these negative values implies that the electron injection process is spontaneous, and its calculated value increases in the order: Dye-R < Dye-2< Dye-1< Dye-3 < Dye-4, we can conclude then injection will occur easily from Dye-4 to the TiO_2 semiconductor, which is in good agreement with the calculated values of E_{ox}^{dye*}. The efficiency of light collection (LHE) is one of the important parameters that can evaluate the performance of the DSSCs. From Table 5, the calculated LHE values for the main absorption peaks of the dyes are in a narrow range of 0.868–0.948, indicating that all the studied dyes give a similar photocurrent. The order of the theoretical performance of these dyes increases as follows: Dye-1< Dye-2< Dye-R < Dye-4< Dye-3.

3.9. IP, EA and reorganization energy

The reorganization energy is one of the significant parameters in the effective charge transfer and photovoltaic conversion of solar cells [72]. Moreover, the larger carrier mobility for any organic compound corresponds to its small reorganization energy [73]. The total reorganization energy (λ_{total}) is the combination of the electron (λ_e) and hole (λ_h) reorganization energies, which can be expressed as follows:

$$\lambda_e = \left(E_n^- - E_a\right) + \left(E_a^0 - E_n\right) \tag{10}$$

$$\lambda_h = \left(E_n^+ - E_c\right) + \left(E_c^0 - E_n\right) \tag{11}$$

$$\lambda_{total} = \lambda_e + \lambda_h \tag{12}$$

where:

Table 7
Absorption data for studied compounds in chloroform ($CHCl_3$) solvent calculated by TD-DFT at CAM-B3LYP/6-31G(d,p) level.

Dye	*Transition character*	*ΔE (eV)*	λ_{max} *(nm)*	*f*
Dye-R	HOMO→LUMO (68%)	2.6944	460.16	1.2353
Dye-1	HOMO→LUMO (49%)	2.9518	420.02	1.9734
Dye-2	HOMO→LUMO (52%)	2.9614	418.67	2.1854
Dye-3	HOMO→LUMO (66%)	2.2712	545.91	1.4452
Dye-4	HOMO→LUMO (66%)	2.2245	557.36	1.3194

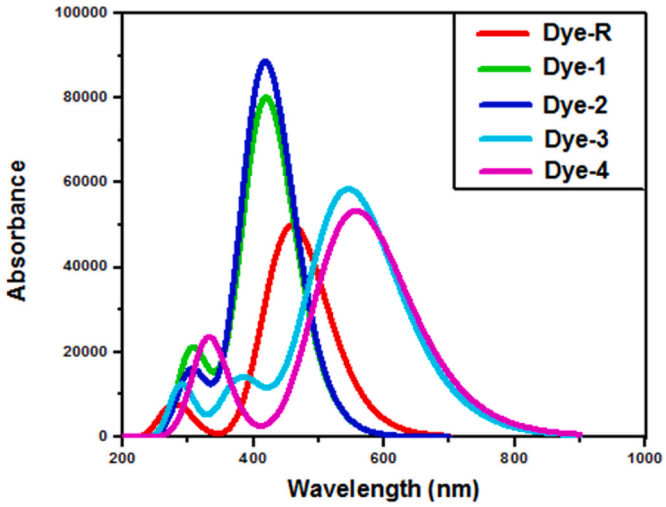

Fig. 8. Simulated absorption spectra of the studied compounds in chloroform ($CHCl_3$) calculated by TD-DFT/CAM-B3LYP/6-31G(d,p) level.

$\mathbf{E_n^-}$, $\mathbf{E_n^+}$ **:** The energy of the anion and cation calculated with the optimized structure of the neutral molecule.
$\mathbf{E_a}$, $\mathbf{E_c}$, $\mathbf{E_n}$ **:** The total energies of the anion, cation and neutral systems at their optimized geometry respectively.
$\mathbf{E_a^0}$, $\boldsymbol{E_c^0}$ The energies of the neutral systems at their optimized cation and anion geometries.

Table 6 presents the calculated, at the DFT-B3LYP/6-31G(d,p) level of the theory, of the energy values of the total reorganization energy (λ_{total}), the reorganization energy of the electron (λ_e) and of the hole (λ_h). We note that the reorganization energies values are smaller and quasi-similar between them indicating that these compounds are a typical electron transport material. Also, the hole reorganization energy (λ_h) values of all the dyes are smaller than those of (λ_e) values except for the Dye-2 compound. Probably due at the addition of the second donor between π-linker and acceptor. it represents that the hole carrier mobility is greater than that of the electron.

Similarly, it is also crucial to calculate the electron affinity (EA) and ionization potential (IP), which characterize the reduction and oxidation properties. These calculations can be calculated using the following equations:

$$IP = E_c - E_n \tag{13}$$

$$EA = E_n - E_a \tag{14}$$

The result of these two parameters is listed in Table 6. As given away in Table 6, we notice that the ionization potential (IP) decrease in following order Dye-R > Dye-3>Dye-4>Dye-1>Dye-2 and on another side the electron affinity (EA) increases in following order Dye-R < Dye-2<Dye-1<Dye-3<Dye-4. As in known, lower IP is beneficial to facilitate hole injection, while higher EA will promote electron injection.

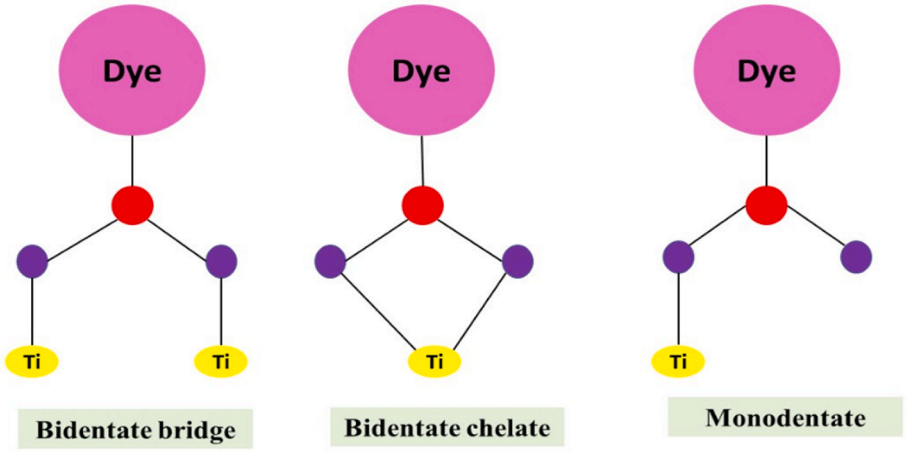

Scheme 1. Possible binding modes for anchoring groups on the TiO_2 surface (carboxylate unit in this case).

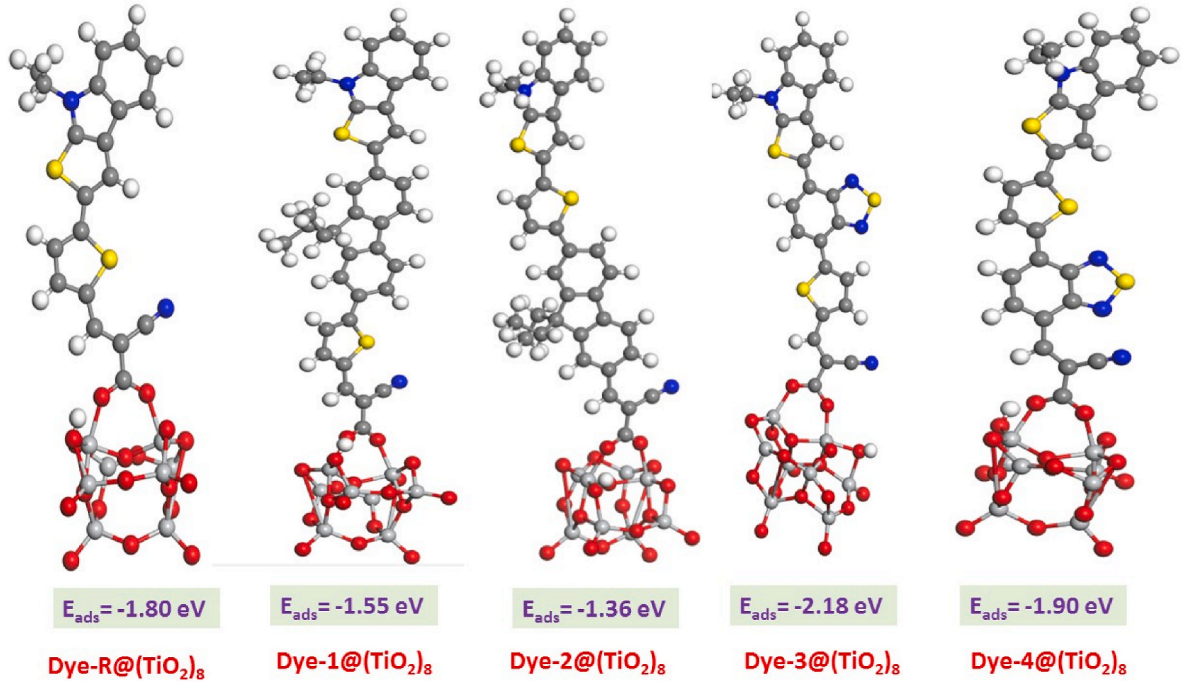

Fig. 9. Ground state optimized geometries of dye-$(TiO_2)_8$ cluster obtained using DMol[3].

3.10. Optical properties of the isolated dyes

We proceed to calculate the maximum wavelength of absorption spectrum (λ_{max}), the vertical excitation energy (ΔE) and corresponding oscillator strength (OS or f). These calculations were simulated using TD-DFT with CAM-B3LYP functional and 6–31 (d, p) basis set. The obtained results are presented in Table 7 and the simulated absorption spectra of the five dyes in chloroform solution are displayed in Fig. 8. According to the values present in Table 7, we note that the values of λ_{max} for all the dyes are sorted in the order Dye-4>Dye-3>Dye-R > Dye-1>Dye-2, which is in excellent agreement with the order corresponding to the values of the energy gaps. On another side, we note that the excitation energy decreases when we introduce the various auxiliary acceptors/donors in the order Dye-2>Dye-1>Dye-R > Dye-3>Dye-4. Fig. 7 shows that the maximum wavelength of absorption spectrum λ_{max} is insensitive to the position of the auxiliary donor in the π-linker, D-D′-π-A/D-π-D′-A. Indeed, λ_{max} of Dye-1 (420 nm) and Dye-2 (418 nm) are almost identical. Unlike the incorporation of an auxiliary acceptor in the π-linker, D-A′-π-A/D-π-A′-A, we notice that the position of this latter affects the value of the λ_{max}. It is more important for D-π-A′-A than for D-A′-π-A, Dye-4 (557 nm)> Dye-3 (545 nm). In general, we can deduce that the addition of an auxiliary acceptor in the π-linker reduces much more the excitation energy of the dye than during the incorporation of an auxiliary donor group. Finally, we note that the Dye-4 molecule has the highest absorption wavelength λ_{max} among these dyes, so that it may have more remarkable properties in the photo-physical domains.

3.11. Electronic and optical properties of the dyes@$(TiO_2)_8$ system

Adsorption of dye plays a very important role in the overall solar energy conversion stabilities and efficiencies of DSSCs [74,75]. As is known, there are many types of adsorption modes such as monodentate, bidentate chelate and bidentate bridge binding modes (Scheme 1). In this paper, we have chosen the bidentate bridge mode because it is considered to be the most stable for the carboxylate [76–78]. the optimized structures of the dyes adsorbed on the surface $(TiO_2)_8$ (101) and

Table 8
Selected bond lengths (Å) of dye/TiO_2 systems.

Dye	Ti–O1	Ti–O2
Dye-R	2.026	2.094
Dye-1	2.011	2.107
Dye-2	2.048	2.082
Dye-3	1.991	1.958
Dye-4	2.036	2.074

the adsorption energies (E_{ads}) are presented in Fig. 9 and the bond distances between the interacting atoms of the dyes and $(TiO_2)_8$ are listed in Table 8.

As shown in Table 8, The bond lengths (Ti–O) between the oxygen (O) atoms of the dyes and the titanium (Ti) of the $(TiO_2)_8$ complex are between 1.958 and 2.107 Å for all dye@$(TiO_2)_8$ complexes. This means that all dyes exhibiting a strong adsorption capacity on the surface of TiO_2.

On the other hand, the adsorption energy (E_{ads}) was calculated using the following expression:

$$E_{ads} = E_{Dye-TiO2} - \left(E_{Dye} + E_{TiO2}\right) \quad (15)$$

where, $E_{Dye-TiO2}$ represents the total energy of the dye complex- $(TiO_2)_8$, E_{Dye} is the total energy of the isolated dye and E_{TiO2} represents the total energy of the group $(TiO_2)_8$. From Fig. 9, we remark that, the adsorption energy (E_{ads}) for all dye/$(TiO_2)_8$ complexes are negative, which is between −1.36 eV and −2.18 eV, which shows that all dyes had stable adsorption. To go further, Dye-2@TiO_2 is the least stable complex with $E_{ads} = -1.36$ eV, while the dyes Dye-3@TiO_2 ($E_{ads} = -2.18$ eV) and Dye-4@TiO_2 ($E_{ads} = -1.90$ eV) are the most stable complexes, they form the strongest bonds with the semiconductor.

3.12. The frontier molecular orbitals (FMOs) of dye/$(TiO_2)_8$ complexes

The frontier molecular orbitals (FMOs) HOMOs and LUMOs of the dye/$(TiO_2)_8$ complexes are very important factors in determining whether the charge transfer that will take place between the donor (Dye-R, Dye-1, Dye-2, Dye-3 and Dye-4) and the acceptor (TiO_2) is effective. From Fig.10, we noticed that, the HOMO of all the dyes is mainly localized on the dye (Dye-R, Dye-1, Dye-2, Dye-3 and Dye-4). While, the electron distributions of LUMO is distributed over the TiO_2 cluster, this means that there is a transfer of donor charge from the designed dyes molecules to the TiO_2 acceptor.

3.13. Optical properties of dye adsorbed onto TiO_2

From the optimized ground state structures obtained using the generalized Perdew-Burke-Ernzerhof (PBE) method with dual digital polarization (DNP) which is the highest quality base set available in DMol^3, we simulated the UV–Vis spectra of the studied dye@TiO_2 systems in the chloroform ($CHCl_3$) solvent based on TD-DFT calculations using the CAM-B3LYP functional and the 6–31 G (d, p) orbital base. The

Table 9
Calculated electronic transition energies (eV), molecular orbital character (MO/character), oscillator strengths (f) and absorption wavelengths (nm) of corresponding electronic transition states of Dye@TiO_2 complexes in chloroform.

Dye	Transition character	ΔE (eV)	λ_{max} (nm)	f
Dye-R	H→L (68%)	2.2182	558.94	0.3991
Dye-1	H→L (49%)	2.2553	549.74	0.2250
Dye-2	H→L (52%)	2.0527	604.02	0.0162
Dye-3	H→L+2 (66%)	1.8005	688.60	2.2852
Dye-4	H→L+2 (66%)	1.8426	672.89	1.8468

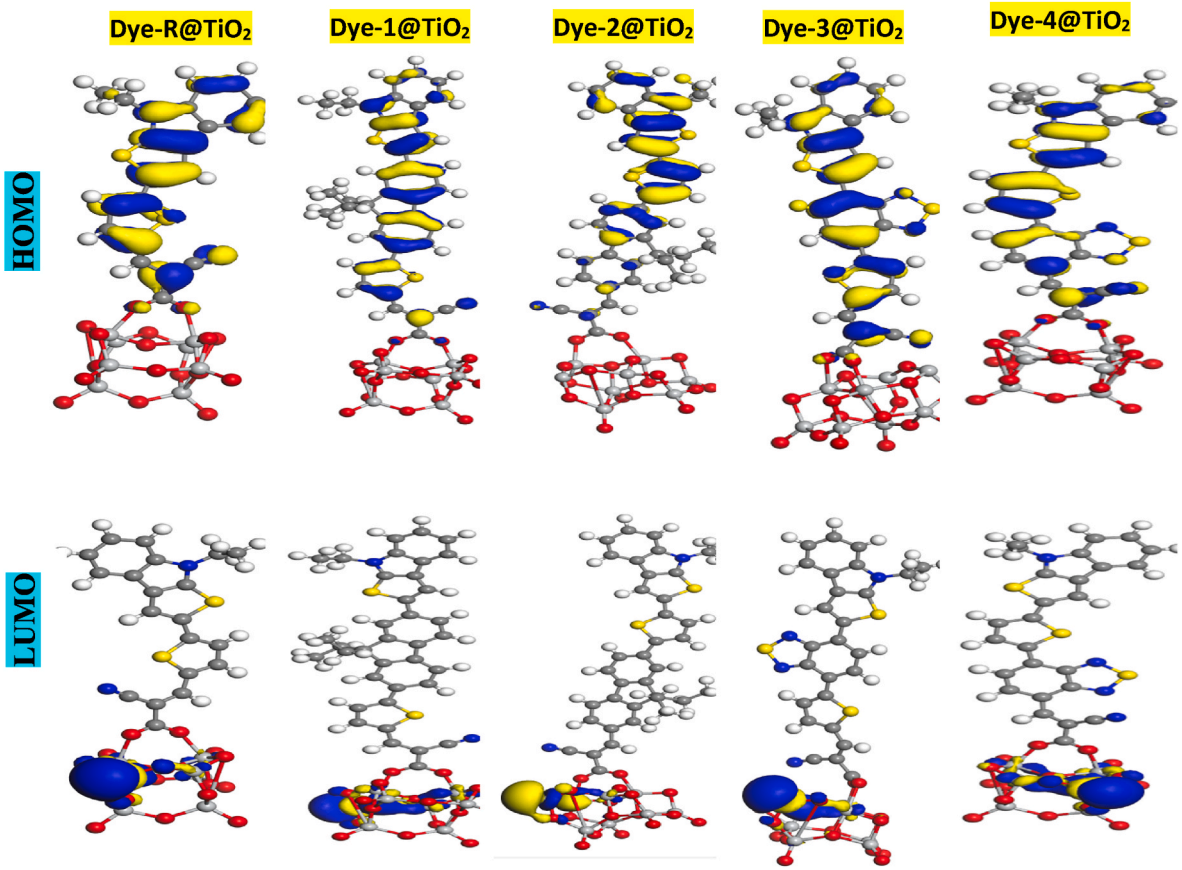

Fig. 10. Simulated frontier molecular orbitals of dye-$(TiO_2)_8$ cluster obtained using DMol^3.

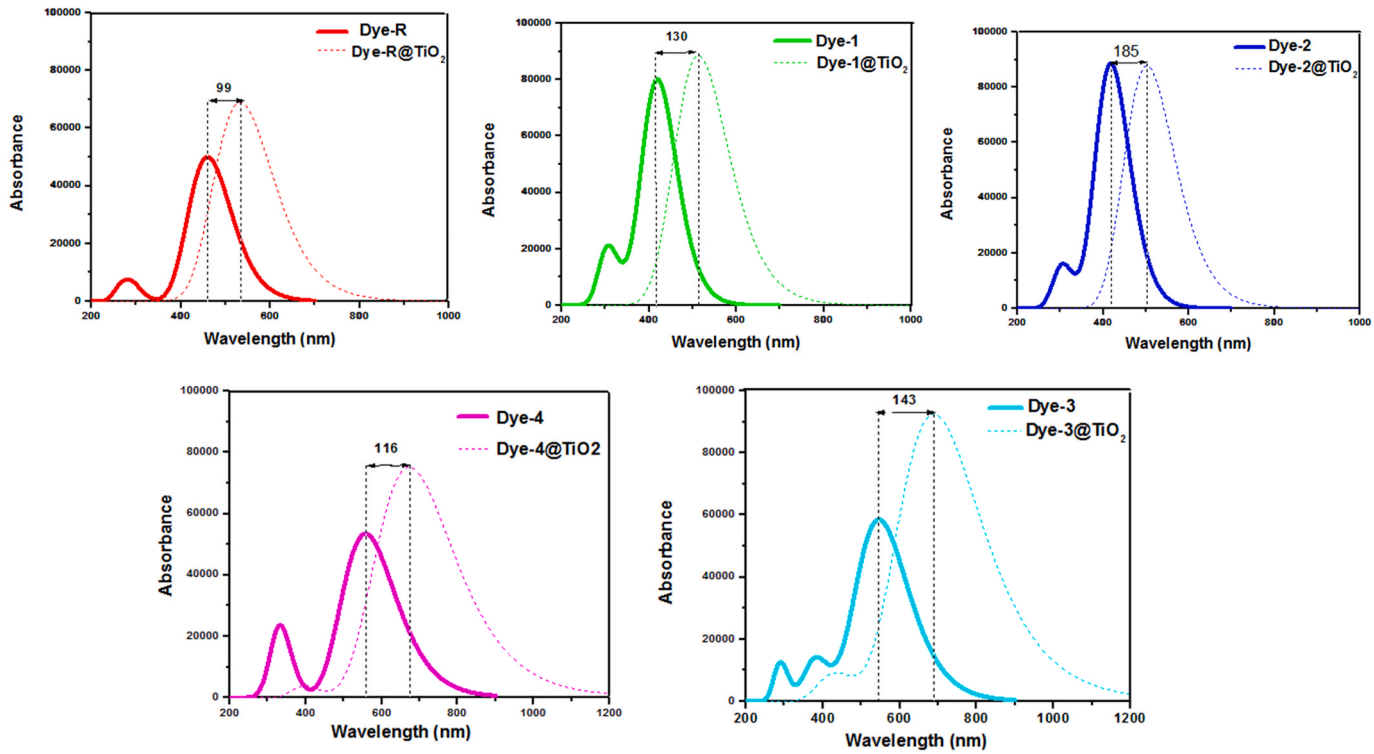

Fig. 11. Absorption spectra of the free dyes and dye@$(TiO_2)_8$ complexes.

excitation energies of first vertical electronic transitions (ΔE), the maximum absorption wavelengths (λ_{max}) and the oscillator forces (f) of all dye@TiO_2 in the presence of the solvent (chloroform), are summarized in Table 9. The simulated absorption spectra obtained at IEF-PCM/TD-CAM-B3LYP/6-31G(d,p) for the studied compounds Dye (Dye-R, Dye-1, Dye-2, Dye-3 and Dye-4) and dye@TiO_2 (Dye-R@TiO_2, Dye-1@TiO_2, Dye-2@TiO_2, Dye-3@TiO_2 and Dye-4@TiO_2)are presented in Fig. 11. From the results we notice that the values of the maximum absorption wavelengths were increased when the dyes bind to the surface of TiO_2. Furthermore, we also remarked that the improvement of the maximum absorption (λ_{max}) between the free dyes and the (dyes@TiO_2) complexes which are between (~99 nm and ~185 nm). We can clearly observe that Dye-3@TiO_2 (688.60 nm) and Dye-4 @TiO_2 (672.89 nm) showed a red shift from the base molecule Dye-R@TiO_2 (558.94 nm), which confirms that the introduction of the acceptor auxiliary into the basic Dye-R compound plays an important role in improving the absorption and adsorption parameters.

4. Conclusion

We have presented a combined DFT, DFTB and TD-DFT studies of five dyes of the family of indole reputed to give good photoconversion in DSSCs. Initially, we used DFT at B3LYP level with the 6-31G (d, p) basis set and DFTB method to optimize the geometry and theoretically compute electrochemical, and photovoltaic properties. Then, we performed TD-DFT at CAM-B3LYP level to examine optical properties of the designed dyes. Our obtained results have shown that the incorporation of the second acceptor, in the π-spacer, gives very good result by comparing with the addition of an auxiliary donor. Furthermore, we noted that this incorporation decreases the E_{gap} value, increases the wavelength value λ_{max} leading to a bathochromic effect on the absorption bands, destabilizes the HOMO level and stabilizes that of LUMO facilitating the injection and the regeneration of electrons. On the other hand, the optimized structures and electronic parameters of the five dye@$(TiO_2)_8$ complexes were investigated by the DFT method, and their optical properties are investigated using TD-DFT. The results show that all of the dyes have stable adsorption and they have wider, red-shifted UV–visible absorption spectra compared to isolated dyes. The analysis of the results of the adsorption shows that the dyes in which an auxiliary acceptor has been incorporated perform better than those which have been grafted with a donor auxiliary. Finally, in view of the photovoltaic results obtained, we can conclude that we have established useful theoretical criteria to improve the efficiency of sensitizers of D-π-A structure based on indole and that the studied compounds seem to have great potentialities for application as a sensitizer in DSSC photovoltaic cells.

Credit author statement

Rahma El Mouhi: Conceptualization, Methodology, Validation, Formal analysis, Investigation, Writing – original draft, Visualization. Ahmed Slimi: Validation, Supervision, Writing – review & editing. Asmae Fitri: Validation, Supervision, Writing – review & editing. Adil Touimi Benjelloun: Validation, Supervision, Writing – review & editing. Souad Elkhattabi: Validation, Supervision, Writing – review & editing. Mohammed Benzakour: Validation, Writing – review & editing. Mohammed Mcharfi: Validation, Writing – review & editing. Mustafa Kurban: Validation, Writing – review & editing.

Declaration of competing interest

The authors declare that they have no known competing financial interests or personal relationships that could have appeared to influence the work reported in this paper.

References

[1] B. O'Regan, M. Gratzel, A low-cost, high-efficiency solar cell based on dye-sensitized colloidal TiO_2 films, Nature 353 (1991) 737–740.
[2] T. Horiuchi, H. Miura, K. Sumioka, S. Uchida, High efficiency of dye-sensitized solar cells based on metal-free indoline dyes, J. Am. Chem. Soc. 126 (39) (2004) 12218–12219.

[3] A. Slimi, M. Hachi, A. Fitri, A. Touimi Benjelloun, S. Elkhattabi, M. Benzakour, M. Mcharfi, M. Khenfouch, I. Zorkani, M. Bouachrine, Effects of electron acceptor groups on triphenylamine-based dyes for dye-sensitized solar cells: theoretical investigation, J. Photochem. Photobiol. Chem. 398 (2020) 112572.
[4] A. Fitri, A. Touimi Benjelloun, M. Benzakour, M. Mcharfi, M. Hamidi, M. Bouachrine, Theoretical studies of the master factors influencing the efficiency of thiazolothiazole-based organic sensitizers for DSSC, J. Mater. Environ. Sci. 7 (3) (2016) 834–844.
[5] M.K. Nazeeruddin, A. Kay, I. Rodicio, R. Humpbry-Baker, E. Miiller, P. Liska, N. V. lachopoulos, M. Grätzel, Conversion of light to electricity by cis-X2bis(2,2'-bipyridyl-4,4'-dicarboxylate)ruthenium(II) charge-transfer sensitizers (X = Cl-, Br-, I-, CN-, and SCN-) on nanocrystalline titanium dioxide electrodes, J. Am. Chem. Soc. 115 (14) (1993) 6382–6390.
[6] L. Schmidt-Mende, J.E. Kroeze, J.R. Durrant, M.K. Nazeeruddin, M. Grätzel, Effect of hydrocarbon chain length of amphiphilic ruthenium dyes on solid-state dye-sensitized photovoltaics, Nano Lett. 5 (7) (2005) 1315–1320.
[7] C.Y. Chen, J.G. Chen, S.J. Wu, J.Y. Li, C.G. Wu, K.C. Ho, Multifunctionalized ruthenium-based supersensitizers for highly efficient dye-sensitized solar cells, Angew. Chem. Int. Ed. 47 (38) (2008) 7452–7455.
[8] A. Abbotto, C. Barolo, L. Bellotto, F. De Angelis, M. Grätzel, N. Manfredi, C. Marinzi, S. Fantacci, J.H. Yum, M.K. Nazeeruddin, Electron-rich heteroaromatic conjugated bipyridine based ruthenium sensitizer for efficient dye-sensitized solar cells, Chem. Commun. 41 (42) (2008) 5318–5320.
[9] J.F. Yin, J.G. Chen, Z.Z. Lu, K.C. Ho, H.C. Lin, K.L. Lu, Toward optimization of oligothiophene antennas: new ruthenium sensitizers with excellent performance for dye-sensitized solar cells, Chem. Mater. 22 (15) (2010) 4392–4399.
[10] A.M. Khudhair, F.N. Ajeel, M.H. Mohammed, Theoretical (DFT and TDDFT) insights into the effect of polycyclic aromatic hydrocarbons on Monascus pigments and its implication as a photosensitizer for dye-sensitized solar cells, J. Microelectr. Eng. 212 (2019) 21–26.
[11] A.A. Youssef, S.M. Bouzzine, Z.M.E. Fahima, İ. Sıdır, M. Hamidi, M. Bouachrine, Designing Donor-Acceptor thienopyrazine derivatives for more efficient organic photovoltaic solar cell: a DFT study, Phys. B Condens. Matter 560 (2019) 111–125.
[12] H.-Y. Chen, J.H. Hou, S.Q. Zhang, Y.Y. Liang, G.W. Yang, Y. Yang, L.P. Yu, Y. Wu, G. Li, Polymer solar cells with enhanced open-circuit voltage and efficiency, Nat. Photonics 3 (2009) 649–653.
[13] A. Le Donne, M. Acciarri, D. Narducci, S. Marchionna, S. Binetti, Encapsulating Eu3 + complex doped layers to improve Si-based solar cell efficiency, Prog. Photovoltaics. 17 (8) (2009) 519–525.
[14] R. Matheu, Ivan A. Moreno-Hernandez, X. Sala, H.B. Gray, B.S. Brunschwig, A. Llobet, N.S. Lewis, Photoelectrochemical behavior of a molecular Ru-based water-oxidation catalyst bound to TiO_2-protected Si photoanodes, J. Am. Chem. Soc. 139 (33) (2017) 11345–11348.
[15] J. Xiao, D. Mei, X. Li, W. Xu, D. Wang, G.L. Graff, W.D. Bennett, Z. Nie, L.V. Saraf, I. A. Aksay, J. Liu, Hierarchically porous graphene as a lithium–air battery electrode, Nano Lett. 11 (11) (2011) 5071–5078.
[16] S. Andoa, J. Nishida, E. Fujiwara, H. Tada, Y. Inoue, S. Tokito, Y. Yamashita, Physical properties and field-effect transistors based on novel thiazolothiazole/heterocyclic and thiazolothiazole/phenylene co-oligomers, Synth. Met. 156 (2–4) (2006) 327–331.
[17] Y. Cui, Y. Wu, X. Lu, X. Zhang, G. Zhou, F.B. Miapeh, W. Zhu, Z.S. Wang, Incorporating benzotriazole moiety to construct D–A−π–A organic sensitizers for solar cells: significant enhancement of open-circuit photovoltage with long alkyl group, Chem. Mater. 23 (19) (2011) 4394–4401.
[18] J. Zhang, Y.H. Kan, H.B. Li, Y. Geng, Y. Wu, Z.M. Su, How to design proper spacer order of the D-π-A dyes for DSSCs? A density functional response, Dyes Pigments 95 (2) (2012) 313–332.
[19] A. Slimi, A. Fitri, A. Touimi Benjelloun, S. Elkhattabi, M. Benzakour, M. Mcharfi, M. Bouachrine, Molecular design of D-π-A-A organic dyes based on triphenylamine derivatives with various auxiliary acceptors for high performance DSSCs, J. Electron. Mater. 48 (2019) 4452–4462.
[20] C. Teng, X. Yang, C. Yang, H. Tian, S. Li, X. Wang, A. Hagfeldt, L. Sun, Influence of triple bonds as π-spacer units in metal-free organic dyes for dye-sensitized solar cells, J. Phys. Chem. C 114 (25) (2010) 11305–11313.
[21] S. Kolemen, O.A. Bozdemir, Y. Cakmak, G. Barin, S. Erten-Ela, M. Marszalek, J. H. Yum, S.M. Zakeeruddin, M.K. Nazeeruddin, M. grätzel, E.U. Akkaya, Optimization of distyryl-bodipy chromophores for efficient panchromatic sensitization in dye sensitized solar cells, Chem. Sci. 2 (5) (2011) 949–954.
[22] S. Ito, S.M. Zakeeruddin, R. Humphry-Baker, P. Liska, R. Charvet, P. Comte, M. K. Nazeeruddin, P. Péchy, M. Takata, H. Miura, S. Uchida, M. Grätzel, High-efficiency organic-dye-sensitized solar cells controlled by nanocrystalline-TiO_2 electrode thickness, Adv. Mater. 18 (9) (2006) 1202–1205.
[23] W. Zhu, Y. Wu, S. Wang, W. Li, X. Li, J. Chen, Z.S. Wang, H. Tian, Organic D-A-π-A solar cell sensitizers with improved stability and spectral response, Adv. Funct. Mater. 21 (4) (2011) 756–763.
[24] R.A. Irgashev, A.A. Karmatsky, S.A. Kozyukhin, V.K. Ivanov, A. Sadovnikov, V. V. Kozik, V.A. Grinberg, V.V. Emets, G.L. Rusinov, V.N. Charushin, A facile and convenient synthesis and photovoltaic characterization of novel thieno[2,3-b] indole dyes for dye-sensitized solar cells, Synth. Met. 199 (2015) 152–158.
[25] R. EL Mouhi, S. El Khattabi, M. Hachi, A. Fitri, A.T. Benjelloun, M. Benzakour, M. Mcharfi, M. Bouachrine, DFT and TD-DFT calculations on thieno[2,3-*b*] indole-based compounds for application in organic bulk heterojunction (BHJ) solar cells, Res. Chem. Intermed. 45 (2019) 1327–1340.
[26] M. Hachi, S. El Khattabi, A. Fitri, A.T. Benjelloun, M. Benzakour, M. Mcharfi, M. Hamidi, M. Bouachrine, DFT and TD-DFT studies of the π-bridge influence on the photovoltaic properties of dyes based on thieno[2,3-b]indole, J. Mater. Environ. Sci. 9 (2018) 1200.
[27] M. Hachi, A. Slimi, A. Fitri, A.T. Benjelloun, S. El Khattabi, M. Benzakour, M. Mcharfi, M. Khenfouch, I. Zorkani, M. Bouachrine, Theoretical design and characterization of D-A1-A based organic dyes for efficient DSSC by altering promising acceptor (A1) moiety, J. Photochem. Photobiol. Chem. 204 (2021) 113048.
[28] F.A. AL-Temimei, L.A. Alasadi, A.S. Alaboodi, DFT study of new donor-π-acceptor materials based on thieno[2,3-b] indole candidate for organic solar cells application, Mater. Sci. Forum 1002 (2020) 221–229.
[29] Z. Wang, H. Wang, M. Liang, Y. Tan, F. Cheng, Z. Sun, S. Xue, Judicious design of indoline chromophores for high-efficiency iodine-free dye-sensitized solar cells, ACS Appl. Mater. Interfaces 6 (8) (2014) 5768–5778.
[30] P. Gao, H.N. Tsao, M. Grätzel, M.K. Nazeeruddin, Fine-tuning the electronic structure of organic dyes for dye-sensitized solar cells, Org. Lett. 14 (17) (2012) 4330–4333.
[31] X. Qian, W.-Y. Chang, Y.-Z. Zhu, S.-S. Wang, B. Pan, L. Lu, J.-Y. Zheng, Tri(N-carbazolyl) triphenylamine-based starburst organic dyes: effects of different acceptors on the optical, electrochemical and photovoltaic properties, RSC Adv. 5 (2015) 47422–47428.
[32] K. Funabiki, H. Mase, Y. Saito, A. Otsuka, A. Hibino, N. Tanaka, H. Miura, Y. Himori, T. Yoshida, Y. Kubota, M. Matsui, Design of NIR-absorbing simple asymmetric squaraine dyes carrying indoline moieties for use in dye-sensitized solar cells with Pt-free electrodes, Org. Lett. 14 (5) (2012) 1246–1249.
[33] W. Li, C. Du, F. Li, Y. Zhou, M. Fahlman, Z. Bo, F. Zhang, Benzothiadiazole-based linear and star molecules: design, synthesis, and their application in bulk heterojunction organic solar cells, Chem. Mater. 21 (21) (2009) 5327–5334.
[34] M.J. Frisch, G.W. Trucks, H.B. Schlegel, G.E. Scuseria, M.A. Robb, J.R. Cheeseman, et al., Gaussian 09, Revision A.02, Gaussian, Inc, Pittsburgh PA, 2009.
[35] R. Dennington, T. Keith, J. Millam, GaussView, Version 5.0, Semichem Inc., Shawnee, 2005.
[36] H. Kurban, M. Dalkilic, S. Temiz, M. Kurban, Tailoring the structural properties and electronic structure of anatase, brookite and rutile phase TiO_2 nanoparticles: DFTB calculs, Comput. Mater. Sci. 183 (2020) 109843.
[37] K. Sun, L. Wang, L. Mao, Y. Zhang, F. Liu, J. Zhang, Influence of π spacer of donor-acceptor-π-acceptor sensitizers on photovoltaic properties in dye-sensitized solar cells, Org. Electron. 76 (2020) 105429.
[38] B. Aradi, B. Hourahine, Th. Frauenheim, DFTB+, a sparse matrix-based implementation of the DFTB method, J. Phys. Chem. A. 111 (26) (2007) 5678–5684.
[39] M. Elstner, D. Porezag, G. Jungnickel, J. Elsner, M. Haugk, Th. Frauenheim, S. Suhai, G. Seifert, Self-consistent-charge density-functional tight-binding method for simulations of complex materials properties, Phys. Rev. B 58 (1998) 7260.
[40] T.A. Niehaus, M. Elstner, Th. Frauenheim, S. Suhai, Application of an approximate density-functional method to sulfur containing compounds, J. Mol. Struct.: THEOCHEM 541 (1–3) (2001) 185–194.
[41] J.P. Foster, F. Weinhold, Natural hybrid orbitals, J. Am. Chem. Soc. 102 (1980) 7211–7218.
[42] N.M. O'Boyle, A.L. Tenderholt, K.M. Langner, cclib: a library for package-independent computational chemistry algorithms, J. Comput. Chem. 29 (2008) 839–845.
[43] A.D. Becke, Density-functional thermochemistry. III. The role of exact exchange, J. Chem. Phys. 98 (1993) 1372.
[44] A.D. Becke, Density-functional exchange-energy approximation with correct asymptotic behavior, Phys. Rev. 38 (1988) 3098.
[45] M. Cossi, V. Barone, Time-dependent density functional theory for molecules in liquid solutions, J. Chem. Phys. 115 (2001) 4708.
[46] C. Adamo, V. Barone, TD-DFT study of the electronic spectrum of s-tetrazine in the gas-phase and in aqueous solution, Chem. Phys. Lett. 330 (2000) 152–160.
[47] M. Hachi, A. Slimi, A. Fitri, S. ElKhattabi, A. Touimi Benjelloun, M. Benzakour, M. Mcharfi, New small organic molecules based on thieno[2,3-b] indole for efficient bulk heterojunction organic solar cells: a computational study, J. Mol. Phys. 118 (8) (2019).
[48] S. Revoju, S. Biswas, B. Eliasson, G.D. Sharma, Phenothiazine-based small molecules for bulk heterojunction organic solar cells; variation of side-chain polarity and length of conjugated system, Org. Electron. 65 (2019) 232–242.
[49] H. Ashassi-Sorkhabi, P. Salehi-Abar, A. Kazempour, Effect of electron-donating groups on the electrochemical and optical properties of indoline substituents as hole transport materials: a computational study, Sol. Energy 180 (2019) 146–151.
[50] B.J. Delley, From molecules to solids with the DMol3 approach, Chem. Phys. 113 (2000) 7756.
[51] H. Etabti, A. Fitri, A.T. Benjelloun, M. Hachi, M. Benzakour, M. Mcharfi, Benzocarbazole-based D–Di–π–A dyes for DSSCs: DFT/TD-DFT study of influence of auxiliary donors on the performance of free dye and dye–Ti_2O interface, Res. Chem. Intermed. 47 (2021) 4257–4280.
[52] J.P. Perdew, K. Burke, M. Ernzerhof, Generalized gradient approximation made simple, Phys. Rev. Lett. 77 (18) (1996) 3865.
[53] N. Benedek, I. Snook, K. Latham, I. Yarovsky, Application of numerical basis sets to hydrogen bonded systems: a density functional theory study, J. Chem. Phys. 122 (14) (2005) 144102.
[54] G.A.M. Mersal, A. Toghan, I.S. Yahia, H.S. El-Sheshtawy, Pyrrole/thiophene π-bridged two triphenylamine electron donor and substituted thiobarbituric electron acceptor for D-π-A-D-featured DSSC applications, J. Chin. Chem. Soc. 68 (10) (2021) 1842–1851.
[55] A. Fitri, A. Touimi Benjelloun, M. Benzakour, M. Mcharfi, M. Hamidi, M. Bouachrine, Theoretical studies of the master factors influencing the efficiency

of thiazolothiazole-based organic sensitizers for DSSC, J. Mater. Environ. 7 (3) (2016) 834–844.
[56] W.L. Ding, D.M. Wang, Z.Y. Geng, X.L. Zhao, W.B. Xu, Density functional theory characterization and verification of high-performance indoline dyes with D–A–π–A architecture for dye-sensitized solar cells, Dyes Pigments 98 (1) (2013) 125–135.
[57] V. Barone, M. Cossi, Quantum calculation of molecular energies and energy gradients in solution by a conductor solvent model, J. Phys. Chem. A. 102 (11) (1998) 1995–2001, 199.
[58] J. Preat, D. Jacquemin, C. Michaux, E.A. Perpète, Improvement of the efficiency of thiophene-bridged compounds for dye-sensitized solar cells, Chem. Phys. 376 (1–3) (2010) 56–68.
[59] J. Zhang, H.B. Li, S.L. Sun, Y. Geng, Y. Wu, Z.M. Su, Density functional theory characterization and design of high-performance diarylamine-fluorene dyes with different π spacers for dye-sensitized solar cells, J. Mater. Chem. 22 (2) (2012) 568–576.
[60] M. Kurban, T.R. Sertbakan, B. Gündüz, A combined experimental and DFT/TD-DFT studies on the electronic structure, structural and optical properties of quinoline derivatives, J. Mol. Model. 26 (6) (2020) 1–7.
[61] M. Snehalatha, C. Ravikumar, I. Hubert Joe, N. Sekar, V.S. Jayakumar, Spectroscopic analysis and DFT calculations of a food additive Carmoisine, Spectrochim. Acta A. 72 (3) (2009) 654–662.
[62] S. Mandal, R. Vedarajan, N. Matsumi, K. Ramanujam, Computational investigation of the influence of p-bridge conjugation order of thiophene and thiazole units in triphenylamine based dyes in dye-sensitized solar cells, J. Chem. Select. 3 (2018) 3582–3590.
[63] J. Tomasi, G. Alagona, R. Bonaccorsi, C. Ghio, R. Cammi, Semiclassical interpretation of intramolecular interactions, Theor. Model. Chem. Bond. (1991) 545–614.
[64] F.J. Luque, J.M. Lopez, M. Orozco, Perspective on "Electrostatic interactions of a solute with a continuum. A direct utilization of ab initio molecular potentials for the prevision of solvent effects", Theor. Chem. Acc. 103 (2000) 343–345.
[65] P. Heng, L. Mao, X. Guo, L. Wang, J. Zhang, Accurate estimation of the photoelectric conversion efficiency of a series of anthracene-based organic dyes for dye-sensitized solar cells, J. Mater. Chem. C 8 (2020) 2388–2399.
[66] W. Fan, W. Deng, Incorporation of thiadiazole derivatives as π-spacer to construct efficient metal-free organic dye sensitizers for dye-sensitized solar cells: a theoretical study, Commun. Comput. Chem. 1 (2013) 152–170.
[67] W. Sang-aroon, S. Saekow, V. Amornkitbamrung, Density functional theory study on the electronic structure of Monascus dyes as photosensitizer for dyesensitized solar cells, J. Photochem. Photobiol., A A. 236 (2012) 35–40.
[68] S. ElKhattabi, M. Hachi, A. Fitri, A. Touimi Benjelloun, M. Benzakour, M. Mcharfi, M. Bouachrine, Theoretical study of the effects of modifying the structures of organic dyes based on N,N-alkylamine on their efficiencies as DSSC sensitizers, J. Mol. Model. 25 (2019) 9.
[69] J.B. Asbury, Y.Q. Wang, E. Hao, H.N. Ghosh, T. Lian, Evidences of hot excited state electron injection from sensitizer molecules to TiO_2 nanocrystalline thin films, Res. Chem. Intermed. 27 (2001) 393–406.
[70] P.F. Barbara, T.J. Meyer, M.A. Ratner, Contemporary issues in electron transfer research, J. Phys. Chem. 100 (31) (1996) 13148–13168.
[71] Z.L. Zhang, L.Y. Zou, A.M. Ren, Y.F. Liu, J.K. Feng, C.C. Sun, Theoretical studies on the electronic structures and optical properties of star-shaped triazatruxene/heterofluorene co-polymers, Dyes Pigments 96 (2) (2013) 349–363.
[72] J. Zhang, H.-C. Zhu, R.-L. Zhong, L. Wang, Z.-M. Su, Promising heterocyclic anchoring groups with superior adsorption stability and improved IPCE for high-efficiency noncarboxyl dye sensitized solar cells: a theoretical study, Org. Electron. 54 (2018) 104–113.
[73] R.A. Marcus, Chemical and electrochemical electron-transfer theory, Rev. Phys. Chem. 15 (1964) 155–196.
[74] W.R. Duncan, O.V. Prezhdo, Theoretical studies of photoinduced electron transfer in dye-sensitized TiO2, Annu. Rev. Phys. Chem. 58 (2007) 143–184.
[75] P. Persson, R. Bergström, S. Lunell, Quantum chemical study of photoinjection processes in dye-sensitized TiO2 nanoparticles, J. Phys. Chem. B 104 (44) (2000) 10348–10351.
[76] M.Y. Mehboob, R. Hussain, M. Adnan, Z. Irshad, M. Khalid, Impact of π-linker modifications on the photovoltaic performance of rainbow-shaped acceptor molecules for high performance organic solar cell applications, Phys. B Condens. Matter 625 (2022) 413465.
[77] M.K. Nazeeruddin, R. Humphry-Baker, P. Liska, M. Grätzel, Investigation of sensitizer adsorption and the influence of protons on current and voltage of a dye-sensitized nanocrystalline TiO2 solar cell, J. Phys. Chem. B 107 (34) (2003) 8981–8987.
[78] Y. Li, P. Song, Y. Yang, F. Ma, Y. Lia, Double-anchoring organic dyes for dye-sensitized solar cells: the opto-electronic property and performance, New J. Chem. 41 (21) (2017) 12808–12829.